

[Click here to view linked References](#)

# **A genome-wide association study implicates the *BMP7* locus as a risk factor for nonsyndromic metopic craniosynostosis**

Cristina M Justice,<sup>1,a</sup> Araceli Cuellar,<sup>2,a</sup> Krithi Bala,<sup>2,a</sup> Jeremy A Sabourin,<sup>1</sup> Michael L Cunningham,<sup>3</sup> Karen Crawford,<sup>4</sup> Julie M Phipps,<sup>4,5</sup> Yan Zhou,<sup>4</sup> Deirdre Cilliers,<sup>5</sup> Jo C Byren,<sup>6</sup> David Johnson,<sup>6</sup> Steven A Wall,<sup>6</sup> Jenny E V Morton,<sup>7,8</sup> Peter Noons,<sup>8</sup> Elizabeth Sweeney,<sup>9</sup> Astrid Weber,<sup>9</sup> Katie E M Rees,<sup>10</sup> Louise C Wilson,<sup>10</sup> Emil Simeonov,<sup>11</sup> Radka Kaneva,<sup>12</sup> Nadezhda Yaneva,<sup>13</sup> Kiril Georgiev,<sup>14</sup> Assen Bussarsky,<sup>14</sup> Craig Senders,<sup>15</sup> Marike Zwienenberg,<sup>16</sup> James Boggan,<sup>16</sup> Tony Roscioli,<sup>17</sup> Gianpiero Tamburrini,<sup>18-19</sup> Marta Barba,<sup>18,20</sup> Kristin Conway,<sup>21</sup> Val C Sheffield,<sup>22</sup> Lawrence Brody,<sup>23</sup> James L Mills,<sup>24</sup> Denise Kay,<sup>25</sup> Robert J Sicko,<sup>25</sup> Peter H Langlois,<sup>26</sup> Rachel K Tittle,<sup>27</sup> Lorenzo D Botto,<sup>28</sup> Mary M Jenkins,<sup>29</sup> Janine M LaSalle,<sup>30</sup> Wanda Lattanzi,<sup>18,20</sup> Andrew O M Wilkie,<sup>4-6</sup> Alexander F Wilson,<sup>1,b</sup> Paul A Romitti,<sup>21,b,c</sup> Simeon A Boyadjiev,<sup>2,b,c</sup> and the National Birth Defects Prevention Study

<sup>a</sup>authors with equal contribution

<sup>b</sup>co-senior authors

<sup>c</sup>co-corresponding authors

## **Affiliations:**

<sup>1</sup>Genometrics Section, Computational and Statistical Genomics Branch, Division of Intramural Research, NHGRI, NIH, Baltimore, MD, USA

<sup>2</sup>Department of Pediatrics, University of California Davis, Sacramento, CA, USA

<sup>3</sup>University of Washington, Department of Pediatrics, Division of Craniofacial Medicine, Seattle Children's Craniofacial Center and Seattle Children's Research Institute, Seattle, WA, USA

<sup>4</sup>MRC Weatherall Institute of Molecular Medicine, University of Oxford, John Radcliffe Hospital, Oxford, UK

<sup>5</sup>Oxford Centre for Genomic Medicine, Oxford University Hospitals NHS Foundation Trust, Oxford, UK

<sup>6</sup>Craniofacial Unit, Oxford University Hospitals NHS Foundation Trust, Oxford, UK

<sup>7</sup>West Midlands Regional Clinical Genetics Service and Birmingham Health Partners, Birmingham Women's and Children's Hospitals NHS Foundation Trust, Birmingham, UK

<sup>8</sup>Birmingham Craniofacial Unit, Birmingham Women's and Children's Hospitals NHS Foundation Trust, Birmingham, UK

<sup>9</sup>Department of Clinical Genetics, Liverpool Women's NHS Foundation Trust, Liverpool, England, UK

<sup>10</sup>Clinical Genetics Service, Great Ormond Street Hospital for Children NHS Foundation Trust, London, UK

<sup>11</sup>National Institute of Pediatrics, Sofia Medical University, Sofia, Bulgaria

<sup>12</sup>Molecular Medicine Center, Department of Medical Chemistry and Biochemistry, Medical Faculty, Medical University of Sofia, Sofia, Bulgaria

<sup>13</sup>National Genetic Laboratory, University Hospital of Obstetrics and Gynecology "Maichin Dom", Medical University of Sofia, Sofia, Bulgaria

<sup>14</sup>Department of Neurosurgery, University Hospital 'St. Ivan Rilski', Medical University of Sofia, Sofia, Bulgaria

<sup>15</sup>Department of Otolaryngology, Head and Neck Surgery, University of California Davis, Sacramento, CA, USA

<sup>16</sup>Department of Neurosurgery, University of California Davis, Sacramento, CA, USA

- <sup>17</sup>Neuroscience Research Australia, University of New South Wales, Sydney, Australia  
<sup>18</sup>Fondazione Policlinico Universitario A. Gemelli IRCCS, Rome, Italy  
<sup>19</sup>Department of Neuroscience, Section of Neurosurgery, Università Cattolica del Sacro Cuore, Rome, Italy  
<sup>20</sup>Department of Life Science and Public Health, Section of Experimental Biology, Università Cattolica del Sacro Cuore, Rome, Italy  
<sup>21</sup>Department of Epidemiology, College of Public Health, The University of Iowa, Iowa City, IA, USA  
<sup>22</sup>Department of Pediatrics, Division of Medical Genetics, Carver College of Medicine, The University of Iowa, Iowa City, IA, USA  
<sup>23</sup>Gene and Environment Interaction Section, NHGRI, NIH, Bethesda, MD, USA  
<sup>24</sup>Epidemiology Branch, Eunice Kennedy Shriver NICHD, NIH, Bethesda, MD, USA  
<sup>25</sup>Division of Genetics, Wadsworth Center, NYS Department of Health, Albany, NY, USA  
<sup>26</sup>Birth Defects Epidemiology and Surveillance Branch, Texas Department of State Health Services, Austin, TX, USA  
<sup>27</sup>Department of Nutritional Sciences, University of Texas at Austin, Austin, TX, USA  
<sup>28</sup>Department of Pediatrics, University of Utah School of Medicine, Salt Lake City, UT, USA  
<sup>29</sup>National Center on Birth Defects and Developmental Disabilities, Centers for Disease Control and Prevention, Atlanta, GA, USA  
<sup>30</sup>Department of Medical Microbiology and Immunology, Genome Center, and MIND Institute, University of California Davis, Davis, CA, USA

#### **Co-corresponding Authors**

Paul A Romitti, PhD  
Department of Epidemiology  
The University of Iowa  
145 N Riverside Dr, S416 CPHB  
Iowa City, IA 52242  
Tel 319-335-4912  
Fax 319-335-4915  
email: [paul-romitti@uiowa.edu](mailto:paul-romitti@uiowa.edu)

Simeon A Boyadjiev, MD  
Department of Pediatrics  
University of California Davis  
4625 2nd Avenue, Research Building II  
Sacramento, CA 95817 USA  
Tel 916-703-0446  
Fax 916-703-0460  
email: [sboyd@ucdavis.edu](mailto:sboyd@ucdavis.edu)

Abstract Word Count=250 (Limit=250)

Main Text Word Count=5,436

## Abstract

Our previous genome-wide association study (GWAS) for sagittal nonsyndromic craniosynostosis (sNCS) provided important insights into the genetics of midline CS. In this study, we performed a GWAS for a second midline NCS, metopic NCS (mNCS), using 215 non-Hispanic white case-parent triads. We identified six variants that were genome-wide significant ( $P \leq 5 \times 10^{-8}$ ): rs781716 ( $P = 4.71 \times 10^{-9}$ ; odds ratio [OR] = 2.44) intronic to *SPRY3*; rs6127972 ( $P = 4.41 \times 10^{-8}$ ; OR = 2.17) intronic to *BMP7*; rs62590971 ( $P = 6.22 \times 10^{-9}$ ; OR = 0.34), located ~155 kb upstream from *TGIF2LX*; and rs2522623, rs2573826, and rs2754857, all intronic to *PCDH11X* ( $P = 1.76 \times 10^{-8}$ , OR = 0.45;  $P = 3.31 \times 10^{-8}$ , OR = 0.45;  $P = 1.09 \times 10^{-8}$ , OR = 0.44, respectively). We performed a replication study of these variants using an independent non-Hispanic white sample of 194 unrelated mNCS cases and 333 unaffected controls; only the association for rs6127972 ( $P = 0.004$ , OR = 1.45; meta-analysis  $P = 1.27 \times 10^{-8}$ , OR = 1.74) was replicated. Our meta-analysis examining single nucleotide polymorphisms common to both our mNCS and sNCS studies showed the strongest association for rs6127972 ( $P = 1.16 \times 10^{-6}$ ). Our imputation analysis identified a linkage disequilibrium block encompassing rs6127972, which contained an enhancer overlapping a CTCF transcription factor binding site (chr20:55,798,821-55,798,917) that was significantly hypomethylated in mesenchymal stem cells derived from fused metopic compared to open sutures from the same probands. This study provides additional insights into genetic factors in midline CS.

**Keywords:** genome-wide association study; nonsyndromic, metopic craniosynostosis; *BMP7*; *SPRY3*; *TGIF2LX*; *PCDH11X*

## Introduction

Craniosynostosis (CS) arises from the premature closure of one or more of the infant cranial vault sutures. This premature closure of the cranial sutures results in intracranial pressure as the infant's brain grows, which can lead to blindness, seizures, and/or brain damage (Gupta et al. 2003; Tamburrini et al. 2005; Thompson et al. 1995). Surgical intervention is required to relieve the intracranial pressure and allow for brain growth. Even after successful surgery, children with CS can experience ongoing medical problems, such as developmental disabilities (Magge et al. 2002) and vision problems (Gupta et al. 2003). Long-term assessment of neurobehavioral outcomes identified learning disabilities (most often language or visual perception deficits) in 47% of affected school-aged children (Kapp-Simon 1998) compared to 10% of unaffected children in the general population (Altarac and Saroha 2007).

Approximately 80% of CS cases are nonsyndromic (NCS) (Cohen and MacLean 2000), where the premature suture fusion is the only major defect. Two common NCS subtypes are sagittal NCS (sNCS) and metopic NCS (mNCS), which affect the midline skull sutures. Estimates for sNCS suggest it occurs in 1.9 - 2.3 per 10,000 live births (Hunter and Rudd 1976; Lajeunie et al. 1996) with a 3:1 male to female ratio (Cohen and MacLean 2000). About 2% of sNCS cases are thought to be familial with an increased recurrence risk of 1% for siblings of affected individuals (Lajeunie et al. 1996). Our previous GWAS for sNCS, consisting of 130 non-Hispanic white (NHW) case-parent triads with sNCS, identified robust associations to loci near *BMP2* (rs1884302;  $P=1.1 \times 10^{-39}$ ; OR=4.38) and within *BBS9* (rs10262453;  $P=5.6 \times 10^{-20}$ ; OR=0.24) (Justice et al. 2012), which were genes not previously reported in CS patients.

Metopic CS, manifesting as trigonocephaly, occurs in about 1 in 15,000 live births (Cohen and MacLean 2000), with most (75%) cases presenting as nonsyndromic (without developmental

delays and/or additional unrelated major structural defects) (Cohen and MacLean 2000; Greenwood et al. 2014). mNCS shows a three-fold excess among males (Lajeunie et al. 1995; Slater et al. 2008), with a family history of metopic synostosis occurring in about 10-15% of mNCS cases (Jehee et al. 2005; Lajeunie et al. 1995). Additional evidence that genetic factors contribute to the etiology of mNCS comes from the difference between concordance ratios (43% vs. 5%) for monozygotic versus dizygotic twins and the increased incidence (6.4%) for CS among first-degree relatives of probands with mNCS (Greenwood et al. 2014; Lajeunie et al. 2005).

Following up on GWAS for sNCS, we performed the first GWAS for mNCS. Case-parent triads were obtained from the International Craniosynostosis Consortium (ICC; <https://health.ucdavis.edu/pediatrics/boyd-genetics-lab/icc.html>) and National Birth Defects Prevention Study (NBDPS) (Reefhuis et al. 2015; Yoon et al. 2001). Using these samples, we investigated genetic variation associated with mNCS. In addition, we conducted a meta-analysis of our mNCS and sNCS GWAS data to identify associated variants common to both types of midline NCS.

## Materials and methods

### Subjects

#### Discovery sample

Our discovery sample was comprised of 410 families, of which 262 were ICC case-parent triads, 13 were ICC multiplex families, and 135 were NBDPS case-parent triads. The enrollment criterion for the study was mNCS in the absence of other unrelated birth defects and/or developmental delays. The presence of mNCS was validated by computerized tomography of the skull or surgical reports. Participants provided whole blood or oral (buccal) specimens. Data collection was approved by the Institutional Review Boards (IRBs) of the University of California, Davis and all

participating institutions in accordance with institutional guidelines. Signed informed consent was obtained for all participants included in the discovery sample. Experimental and data analysis protocols are available upon request from the authors; data has been deposited in database of Genotypes and Phenotypes (dbGaP).

### Replication sample

We selected an independent non-Hispanic white (NHW) sample of 285 unrelated cases and 855 unaffected controls for replication. Case and control specimens either were mother-child dyads recruited from the ICC or NBDPS or from anonymized residual newborn blood spots provided by the New York State Department of Health where the proband had a diagnosis of mNCS confirmed by the New York State Congenital Malformations Registry. Signed informed consent was obtained for ICC or NBDPS dyads, and IRB approval was obtained from the New York State Department of Health for use of anonymous blood spots.

### Genotyping

#### Discovery sample

We extracted genomic DNA from 688 whole blood and 320 oral specimens and from whole genome amplified DNA from 13 blood and four oral specimens. We performed targeted mutation analysis for *FGFR1*, *FGFR2*, *FGFR3*, and *TWIST1* to exclude mild or atypical syndromic cases (Lattanzi, et al. 2017). The Center for Inherited Disease Research (CIDR) genotyped the specimens using the Infinium Multi-Ethnic Genotyping Array plus DrugDev (MEGA) Array containing 1,881,804 single nucleotide polymorphisms (SNPs), which included 166,523 pharmacogenetic SNPs to assess exposure to medications as a risk factor for mNCS. Genotypes for 1,881,804 SNPs were released for 1,050 specimens, which included 23 blind duplicates and 19 HapMap controls (10 Utah residents of European ancestry, four Han Chinese, two Japanese, three Yorubans). The

1  
2  
3  
4 missing rate was 0.24%, blind duplicate reproducibility rate was 99.99%, and HapMap  
5  
6 concordance rate was 99.70%. We used Plink v1.90b5.2 (Purcell et al. 2007) to detect  
7  
8 discrepancies between expected and annotated sex; five specimens annotated as ‘unknown’ were  
9  
10 reclassified to reflect the genetically-inferred sex. We also used Plink v1.90b5.2 (Purcell et al.  
11  
12 2007) to conduct pairwise identity-by-descent analyses. Three contaminated specimens, three  
13  
14 identified monozygotic twins, 16 siblings, two case-parent triads with inconsistent parent-child  
15  
16 relationships, and 22 cases with additional suture involvement were excluded prior to analysis.  
17  
18  
19  
20

## 21 **Replication sample**

22  
23 Our replication sample was genotyped using a panel of 120 SNPs. The SNPs selected were: 1)  
24  
25 significant at a suggestive genome-wide level in our GWAS ( $P < 1 \times 10^{-5}$ ); 2) part of the Infinium  
26  
27 DrugDev Array and had a  $P < 1 \times 10^{-4}$  because these SNPs had lower MAFs than most other SNPs  
28  
29 in the array; 3) associated with sNCS in our previous GWAS but not with mNCS (at  $P < 1 \times 10^{-5}$ );  
30  
31 or 4) in high linkage disequilibrium (LD) to associated SNPs. Additionally, the replication SNP  
32  
33 panel included 48 Ancestry Informative Markers (AIMs) (Kosoy et al. 2009). CIDR performed  
34  
35 genotyping of the replication sample using TaqMan OpenArray, and genotypes for 115 SNPs (5  
36  
37 SNPs failed genotyping) for 920 specimens were released. These specimens included 18 blind  
38  
39 duplicates (blind duplicate reproducibility rate of 99.4%), 24 HapMap controls (concordance rate  
40  
41 of 99.5%), and 15 replicate specimens, comprised of five case-parent triads from the discovery  
42  
43 sample. SNPs in the replication panel were dropped if they had a call rate  $< 90\%$ , were discordant  
44  
45 in one or more duplicates, or were discordant in any replicate when compared to the GWAS  
46  
47 genotypes. Sixty-six SNPs remained for replication analysis, of which 22 were AIMs.  
48  
49  
50  
51  
52  
53  
54  
55

## 56 **Data analysis**

### 57 **Discovery sample**

We performed principal components analysis (PCA) using the 'prcomp' package in R v3.2.5 on 58,725 SNPs with a minor allele frequency (MAF) > 15% genotyped in all specimens, including the 19 HapMap specimens; SNPs were pruned such that the maximum  $r^2$  within a 50kb sliding window was 0.2. Families with both founders within one standard deviation of PC1 and PC2 of the mean of the 10 HapMap CEU (Utah residents of European ancestry) specimens were retained for analysis. To minimize loss of power, families in which one founder and their affected offspring were within the desired PCA region and the other parent was close to the HapMap CEU cluster were included.

We conducted a genome-wide association test using the allelic transmission disequilibrium test (TDT) as implemented in Plink v1.90b5.2 (Purcell et al. 2007) which analyzed autosomal and chromosome X markers. The TDT was performed on 215 NHW case-parent triads on 650,848 SNPs that met stringent quality-control procedures and had a MAF > 5%. SNPs were dropped if they had a call rate less than 98%, had a Mendelian inconsistency in more than one case-parent triad, were discordant in one or more duplicates, had heterozygous haploid genotypes present, were monomorphic and/or showed deviation from Hardy-Weinberg equilibrium  $P \leq 1 \times 10^{-6}$  (calculated using only the unrelated individuals of European ancestry), or had a MAF difference > 0.20 between males and females on the X chromosome. All SNP map position information was based on Human February 2009 GRCh37/hg19 Assembly. Manhattan and qq-plots were generated using 'qqman' package R v3.23.0 and LD plots were obtained using Haploview v4.234.

The TDT under additive, dominant, and recessive modes of inheritance was performed using the 'trio' R package v3.23.0 (Schwender et al. 2014). A search for two-way gene-gene interactions was carried out using the 'trio' R package v3.23.0 (Schwender et al. 2014) using Cordell's method (Cordell 2002) on 822 selected SNPs. A genotypic TDT for the possible



1  
2  
3  
4 interaction between each pair of SNPs (581,322 tests) was performed, excluding results from SNP  
5  
6 pairs on the same chromosome due to long-range LD. As recommended in Cordell's method  
7  
8 (Cordell 2002), for each case-parent triad, 15 pseudo controls matched to each case were generated  
9  
10 as a function of the parental genotypes of the SNP pair tested. Pseudo controls for each case were  
11  
12 comprised of one of the possible two-locus genotypes that was not transmitted to the case. Using  
13  
14 these 15 pseudo controls and matched cases, a conditional logistic regression model was fitted to  
15  
16  
17  
18 test for epistatic interactions that incorporate additive effects at the two loci.  
19  
20

21 We performed pathway analysis using the SNPs associated with mNCS at  $P < 1 \times 10^{-5}$ , for  
22  
23 which autosomal SNPs were annotated to genes using wANNOVAR (Chang and Wang 2012); X-  
24  
25 linked SNPs were annotated to genes using UCSC Genome Browser (GRCh37/hg19,  
26  
27 [www.genome.ucsc.edu](http://www.genome.ucsc.edu)). Using Ingenuity Pathway Analysis (IPA, QIAGEN, Redwood City,  
28  
29 [www.qiagen.com/ingenuity](http://www.qiagen.com/ingenuity)), we implemented canonical pathway analysis to identify the most  
30  
31 significant pathways from the IPA library of canonical pathways in the annotated genes, and a  
32  
33 Benjamini-Hochberg multiple comparison adjustment was applied (Benjamini and Hochberg  
34  
35 1995). In order to corroborate our results, we used a second pathway analysis program  
36  
37 iGSEAvGWASv1.1 (<http://gsea4gwas.psych.ac.cn/docs/documents.jsp>).  
38  
39  
40  
41  
42

43 A pre-phasing approach was used to impute unobserved SNPs. Genomic strand  
44  
45 information was used to identify and flip the strand of SNPs where the TOP (indicates the A or T  
46  
47 allele containing strand) alleles were not aligned to the plus (“+”) strand of the human genome  
48  
49 reference assembly. Data were phased using SHAPEIT2 (Delaneau et al. 2013), inputting the  
50  
51 filtered, chromosome-specific Plink files and receiving the best guess haplotypes as output. These  
52  
53 best guess haplotypes were fed directly into the minimac3 software (Das et al. 2016) on the  
54  
55 University of Michigan Imputation server, v.1.0.3. The Haplotype Reference Consortium (HRC)  
56  
57  
58  
59  
60  
61  
62  
63  
64  
65

reference panel (McCarthy et al. 2016), which contains 64,976 haplotypes and 39,235,157 sites, was used to filter SNPs with a minor allele count of at least five. The imputation of the pseudo-autosomal regions on chromosomes X and Y, PAR1, and PAR2 could not be carried out on the imputation server; instead, the PAR regions of the X chromosome regions were fed directly into the IMPUTE2 imputation software (Howie et al. 2011) using the 1000 Genomes Project Phase 3 reference panel. Imputed variants were filtered by imputation quality score  $R_{sq} > 0.3$ .

### Replication sample

To analyze our replication sample, we performed PCA using Plink v1.90b5.2 (Purcell et al. 2007) in two stages. The first stage used all 214 cases and 560 controls (including the six HapMap specimens) and identified 201 cases and 533 controls (including three HapMap specimens) within 2.5 standard deviations of the mean of PC1 and PC2. To ensure the selected set of 201 cases and 530 controls (excluding the three HapMap specimens) was homogeneous, PCA was performed again with the 22 AIMs remaining after quality control procedures to identify any remaining structure. Because some population structure was still present, cases and controls within 2.5 standard deviations of the mean of PC1 and PC2 were again selected, yielding 194 cases and 502 controls for analysis.

In order to match the 3:1 male:female ratio observed in the 194 cases, a random selection of female controls that would match this ratio was performed ten times. No significant changes were detected when running association analyses on these ten sets of female controls; thus, one of these selected groups of female controls was randomly selected for the final analysis. This exclusion reduced the number of controls analyzed to 333. For the replication analysis, we applied a  $\chi^2$  test for allelic association using Plink v1.90b5.2 (Purcell et al. 2007). This test does not adjust for covariates, such as sex; thus, the sample with a reduced number of female controls was used. Our

association results ( $P$  value) for the 10 sets of samples for which females were randomly dropped to match the 3:1 ratio found in the cases are presented in Table S1. This approach was selected rather than applying logistic regression analysis, which could adjust for sex, because the meta-analysis method that was used applied a  $\chi^2$  test (Kazeem and Farrall 2005).

## Meta-analyses

### Discovery and replication samples

We conducted a meta-analysis combining the results from our discovery TDT and replication case-control study using a fixed-effects model, which tested for interstudy heterogeneity (Kazeem and Farrall 2005). We also conducted a meta-analysis of our previous sNCS and mNCS GWAS data. In the meta-analysis, imputation of the mNCS data to match the genotyped sNCS specimens was considered, but because of discrepancies between imputed and genotyped variants due to differences in allele frequencies between the reference panels and the small sample size available, it was preferable to only use the genotyped variants in both studies. The sNCS GWAS was genotyped using the Illumina 1 M Human Omni1-Quad array (Justice et al. 2012), and LiftOver (Kent et al. 2002) was used to convert all hg18 positions to hg19 positions. Chromosome and base pair (bp) position SNPs from the sNCS GWAS were compared to those on the Illumina MEGA array used in the mNCS GWAS; after removing SNPs with three alleles and those with a MAF < 1%, 306,233 SNPs were retained for the meta-analysis.

## Functional analysis

### Cell culture

Mesenchymal stem cells (MSCs) and HeLa cells were cultured in Dulbecco's modified Eagle's medium supplemented with 10% fetal bovine serum. Culture medium was collected for enzyme-linked immunosorbent assay (ELISA), and MSCs were lysed using Pierce RIPA Buffer (Thermo

Scientific) with protease and phosphatase inhibitors in addition to EDTA and frozen until needed for western blotting.

### **Real-time quantitative polymerase chain reaction**

RNA was isolated from MSCs derived from fused and open sutures using the Zymo RNA Mini-Prep Kit. Real-time quantitative polymerase chain reaction (qPCR) for *BMP7* gene expression analysis was performed using the TaqMan RNA to Ct 1-Step Kit (ThermoFisher). The PCR program began with a 15-minute reverse transcription step at 48° C and a 10-minute activation of the deoxyribonucleic acid (DNA) polymerase at 95° C. This was followed by 40 cycles of denaturation for 15 seconds at 95° C and annealing/extending for one minute at 60° C. TaqMan gene expression assays (ThermoFisher) were used for either *BMP7* (Hs00233476\_m1) or the housekeeping gene *GAPDH* (Hs99999905\_m1). All qPCR reactions were performed in triplicate, and the amplified signals from *BMP7* were normalized to those obtained from *GAPDH* in the same reactions.

### **Exon analysis**

DNA was extracted from blood, saliva, or mouthwash of 183 mNCS patients according to the manufacturer's protocol using the Gentra Puregene Blood Kit (QIAGEN). The KAPA2G Robust HotStart PCR Kit (Kapa Biosystems) was used to amplify the coding exons of *BMP7* gene using the following PCR primers:

BMP7\_exon1\_Forward: CGTCTGCAGCAAGTGACC

BMP7\_exon1\_Reverse: CTGCGATTTCAGCCAGGAG

BMP7\_exon2\_Forward: GATGCTTGGACTCAGAGCC

BMP7\_exon2\_Reverse: GTGCCAATCTGACCCATCC

BMP7\_exon3\_Forward: GATGTTCCCACTTGTCGGG

1  
2  
3  
4 BMP7\_exon3\_Reverse: TGAAGTCCAGGAGCACAGG  
5

6  
7 BMP7\_exon4\_Forward: AACAGTACCTGGCCTAGAGT  
8

9 BMP7\_exon4\_Reverse: GGATTTGGGGGTTTTCTTCC  
10

11 BMP7\_exon5\_Forward: CCGTCTGTGCTTCATTGCT  
12

13  
14 BMP7\_exon5\_Reverse: AGCGAGGCCACTTGATACT  
15

16 BMP7\_exon6\_Forward: TGCTCAGAAGGCATGGTCT  
17

18 BMP7\_exon6\_Reverse: ATGACATGGCAATGGGCTG  
19

20  
21 BMP7\_exon7\_Forward: TAGAACAGGGAGTGCTTGG  
22

23 BMP7\_exon7\_Reverse: AAAGTTGGGGATAGGGAGG  
24

25  
26 PCR products were purified using ExoSap-IT (Affymetrix) and sequenced by Sanger sequencing.  
27

28  
29 Electropherograms were analyzed with the SnapGene software by two independent investigators.  
30

### 31 **Western-blot analyses** 32

33 Equal amounts of protein were heated to 70°C for 10 minutes with NuPAGE LDS Sample Buffer  
34

35 (4×) (Life Technologies), ran on NuPAGE Novex 4–12% Bis-Tris gels (Life Technologies), and  
36

37 transferred to polyvinylidene difluoride membranes (Life Technologies). Membranes were  
38

39 blocked for one hour at room temperature with 5% nonfat milk in Tris Buffered Saline with Tween  
40

41 (TBST; 20 mM Tris-HCl, pH 7.5, 137 mM NaCl, 0.1% Tween 20). Following this, membranes  
42

43 were incubated with primary antibody overnight in blocking solution at 4°C with slight agitation.  
44

45 Primary antibodies for BMP7 (Abcam), phospho-Smad1/5/8 (Cell Signaling), Smad1 (Cell  
46

47 Signaling) and  $\beta$ -tubulin (Cell Signaling) were diluted according to manufacturer's  
48

49 recommendations. The membranes were washed with TBST and incubated with secondary  
50

51 antibody for one hour at room temperature. The secondary antibody (polyclonal goat anti-rabbit  
52

53 immunoglobulins/horseradish peroxidase, ThermoFisher) was diluted according to manufacturer's  
54  
55  
56  
57  
58  
59  
60  
61  
62  
63  
64  
65

recommendations in blocking solution. Membranes were washed with TBST and developed with SuperSignal West Pico PLUS Chemiluminescent Substrate (Thermo Scientific). Experiments were performed in triplicate, and .tiff images were analyzed using ImageJ (<https://imagej.nih.gov/ij/>). Bands were quantified and intensities were normalized with  $\beta$ -tubulin.

### **Enzyme-linked immunosorbent assay**

Levels of secreted BMP7 were measured by an indirect enzyme-linked immunosorbent assay (ELISA). MSCs and HeLa cells were seeded at  $1 \times 10^6$  cells in 100 mm plates and incubated for 24 hours. The media was removed and replaced with serum-free media. The plates were incubated for four hours and the serum-free media was collected. Ninety-six-well microtiter plates were coated with lectin and blocked for two hours at room temperature with 5% nonfat milk in phosphate-buffered saline (PBS). After removing the blocking buffer, the plates were washed with PBS with 0.05% Tween 20. Specimens were added, and the plates were incubated for two hours at room temperature. After washing out unbound substances, a BMP7 monoclonal detective antibody (R&D Systems) was added to the wells and incubated overnight. Again, unbound substances were washed out and the secondary antibody (polyclonal goat anti-mouse, ThermoFisher) was added to the wells. Any unbound antibody-enzyme reagent was washed out and a substrate solution was added to the wells. This caused color development in proportion to the amount of BMP7 present in the specimen. The absorbance of each well was read with an ELISA plate reader (BioTek Synergy HT) at 450 nm. Using a standard curve, the amount of protein secreted by the MSCs and HeLa cells was calculated, and the latter value was used to normalize the data to compare across the different plates.

### **Dual luciferase assay**

We generated 667-bp fragments (chr20:55,796,885-55,797,557, hg19) with the different alleles (G and T) of rs6127972 by PCR using DNA from homozygotes with either allele using primer set: 5'-GAGGGGTGGGCAGGGATAA-3' and 5'-GTTCCGCTTGGGGTCCTC-3'. These fragments were placed in the *SacI/MluI* site of pRLuc-promoter vector (SwitchGear Genomics) upstream of the *BMP7* promoter using the In-Fusion HD Cloning Plus CE kit (Takara Bio USA, Inc.) with primer set: 5'-ACTGGCCGGTACCTGGAGGGGTGGGCAGGGATAAG-3' and 5'-GCTTCCTGGAACGCGTTCCGCTTGGGGTCCTCTC-3'. The resulting constructs (pRLuc-BMP7) contained either the G (common) allele or T (risk) allele. The inserted portions of the resulting constructs were sequenced to verify the nucleic acid sequences and the identity and location of the SNP. For the luciferase assay,  $5 \times 10^3$  HeLa cells were seeded per well in 96-well plates and transfected with an empty vector or with pRLuc-BMP7 containing the risk (T) or common (G) allele using FuGENE HD reagent (Active Motif). pTK-CLuc construct (SwitchGear Genomics) was co-transfected as a normalizing internal control vector. All transfections were carried out in triplicate. After 24 hours of incubation, luciferase activity was measured using the LightSwitch Dual Assay System (SwitchGear Genomics). Each transfection set included the empty control vector, risk allele, and common allele and was performed independently 12 times.

An independent dual-luciferase assay was conducted using randomly selected 667 bp fragments (chr10:45,032,341-45,033,007, hg19) with either the G or T allele of rs1857502. Fragments were placed in the *SacI/MluI* site of pRLuc-promoter vector upstream of the *BMP7* promoter with primer set: 5'- ACTGGCCGGTACCTGCACCATCCAGTCTGTGTC -3' and 5'-GCTTCCTGGAACGCGTTCAATAATCATATCATTGGAGA-3'. Each transfection set included the empty control vector, G allele, and T allele and was performed independently 10 times.

## Pyrosequencing assay

Genomic DNA isolated from 24 MSC lines derived from fused metopic and control open sutures from the same proband (12 of each type) was bisulfite converted using the Zymo EZ DNA-Methylation Lightning Kit. PCR and sequencing primers were designed using the PyroMark Assay Design Software 2.0 (Qiagen). Two sets of pyrosequencing PCR and sequencing primers were designed to cover seven CpG sites (chr20:55,798,821-55,798,917, chr20:55,798,975-55,799,053, hg19). These sites each overlap an enhancer predicted to be active in osteoblasts (chromHMM imputed data) and a CTCF transcription factor binding site. Primers were also designed to cover four CpG sites (chr20:55,796,275-55,796,368, hg19) in a nearby region not overlapping the enhancer and CTCF binding site to serve as a control. The specimens were run in triplicate for all assays. The PyroMark PCR Kit (Qiagen) was used to amplify the bisulfite converted DNA, using the following primers:

CpG1-4-PCR-Forward: 5'- AGAAGTTTAAATTATAGGGTGGAGAT-3'

CpG1-4-PCR-Reverse: 5'-CTTACCCAATCCTCTCCTAAAAATAC-3'

CpG5-7-PCR-Forward: 5'- TTAGGAGAGGATTGGGTAAGGA-3'

CpG5-7-PCR-Reverse: 5'- ACCTTTCTAAAAAACTCCCTAA-3'

Control-PCR-Forward: 5'-ATTGTTTTTGTGTTGGGTTTTATTTAGAT-3'

Control-PCR-Reverse: 5'- AACCAATAACCTACCCAACCTATC-3'

The specimens were sequenced using the PyroMark Biotage Q96 (Qiagen). The following sequencing primers were used:

CpG1-4-Sequencing: 5'- TTTTAATTATAGGGTGGAGATA-3

CpG5-7-Sequencing: 5'- GGATTGGGTAAGGAG – 3'

Control-Sequencing: 5'- GTTTAGTAAGTGTGTTTATATGTTG-3'



## Results

Six SNPs exceeded the genome-wide significance threshold of  $P \leq 5 \times 10^{-8}$  (Figure 1, Figure 2, Figure S1): rs781716 intronic to *SPRY3* ( $P = 4.71 \times 10^{-8}$ ), rs6127972 intronic to *BMP7* ( $P = 4.411 \times 10^{-8}$ ), rs62590971 located 155 kb upstream from *TGIF2LX* ( $P = 6.22 \times 10^{-9}$ ), and three SNPs intronic to *PCDH11X* (rs2522623,  $P = 1.76 \times 10^{-8}$ ; rs2573826,  $P = 3.31 \times 10^{-8}$ ; rs2754857,  $P = 1.09 \times 10^{-8}$ ). Because Plink TDT analysis assumes a multiplicative mode of inheritance by performing an allelic TDT analysis, we also conducted a genotypic TDT analysis using the ‘trio’ R package v3.23.0 (Schwender et al. 2014) to test for additive, dominant, and recessive modes of inheritance. Our results indicated the effect of the significant SNPs was consistent with an additive model (Table S2).

We tested for two-way gene-gene interactions using 822 selected SNPs. Of these, 808 SNPs were located in CS candidate genes (Lattanzi et al. 2017), 13 SNPs had a  $P < 1 \times 10^{-5}$  for the TDT GWAS and were not located in CS candidate gene regions, and one SNP, rs1884302 (345 kb downstream of *BMP2*) identified in our previous GWAS for sagittal NCS (sNCS) (Justice et al. 2012), was not significant in our current study (Table S3). No significant interaction effect was observed after correcting for multiple testing (581,322 tests, Bonferroni  $P < 9 \times 10^{-8}$ ), with the most significant association ( $P = 1.16 \times 10^{-5}$ ) observed for an interaction between rs876688 (intronic to *TGFBR2*) and rs4637716 (intronic to *BBS9*). Pathway analysis conducted by selecting SNPs associated with mNCS in the 215 NHW case-parent triads at  $P < 1 \times 10^{-5}$  did not show any pathways to be enriched at a Benjamini-Hochberg false discovery rate of 0.05.

We extracted the imputed regions ( $\pm 100$  kb) on each chromosome (2, 5, 11, 20) where there were suggestive genome-wide significant associations ( $P < 1 \times 10^{-5}$ ) and the PAR2 pseudo-autosomal region on the X chromosome. Genome-wide significant associations for SNPs were

1  
2  
3  
4 identified only on chromosome 20 intronic to *BMP7*. The most significant association was for  
5  
6 rs162319 ( $P = 2.86 \times 10^{-8}$ , Figure S2), which was comparable to the genotyped rs6127972 ( $P =$   
7  
8  $4.41 \times 10^{-8}$ ).  
9

10  
11 Our replication analyses included markers on the X chromosome, which are susceptible to  
12  
13 type 1 errors when allelic frequencies differ between males and females in an unbalanced sample  
14  
15 (different number of females and males in cases vs. controls) (Loley et al. 2011). As such, a random  
16  
17 sample of females was selected and dropped from the control sample to match the 3:1 male:female  
18  
19 ratio observed in the 194 cases and reduced the number of controls analyzed to 333. The only SNP  
20  
21 which was genome-wide significant in our discovery sample and replicated in our case-control  
22  
23 sample was rs6127972 ( $P = 0.004$ , OR = 1.45).  
24  
25  
26  
27

28  
29 In our meta-analysis combining the results from our discovery TDT and the replication  
30  
31 case-control study, the only genotyped SNP to reach genome-wide significance was rs6127972 ( $P$   
32  
33  $= 1.27 \times 10^{-8}$ ). SNPs identified at a suggestive genome-wide significance level ( $P < 1 \times 10^{-5}$ )  
34  
35 included rs10254116, rs10262453, and rs4723276 in *BBS9*; rs34360385 ~ 282kb and ~627kb from  
36  
37 *PABC5* and *TGI2LX*, respectively; and rs230217, rs6014954, rs230218, and rs17404303, in close  
38  
39 proximity to rs6127972 (Table S4), with the imputed SNPs rs4723276, rs230217, rs6014954, and  
40  
41 rs230218 reaching genome-wide significance ( $P < 5 \times 10^{-8}$ ).  
42  
43  
44

45  
46 Combining data for genotyped SNPs (MAF > 1%) common to our GWAS for mNCS and  
47  
48 our previous GWAS for sNCS, we performed a meta-analysis with the 215 NHW mNCS and 130  
49  
50 NHW sNCS case-parent triads (Justice et al. 2012) using METAL (Willer et al. 2010). No SNP  
51  
52 reached genome-wide significance, with the top association identified for rs6127972 ( $P = 1.16 \times$   
53  
54  $10^{-6}$ ). For SNPs rs1884302 and rs10262453, the most significant associations found in our previous  
55  
56 sNCS GWAS, only rs10262453 reached a significance level of  $P < 1 \times 10^{-5}$  in both our mNCS  
57  
58  
59  
60  
61  
62  
63  
64  
65

1  
2  
3  
4 GWAS and sNCS GWAS. Opposite directions of effect were observed for rs10262453, with the  
5  
6 A allele being over-transmitted for sNCS, but the C allele being over-transmitted for mNCS (Table  
7  
8 S5). This finding may indicate a functional role for this variant.  
9

10  
11 We sequenced all seven exons of *BMP7* in 183 NHW mNCS cases, of which 118 were  
12 included in our discovery sample. No variation from the reference coding sequence of the gene  
13 was observed. Because no deleterious *BMP7* mutations (loss of function or missense variants)  
14 was observed. Because no deleterious *BMP7* mutations (loss of function or missense variants)  
15 was observed. Because no deleterious *BMP7* mutations (loss of function or missense variants)  
16 was observed. Because no deleterious *BMP7* mutations (loss of function or missense variants)  
17 was observed. Because no deleterious *BMP7* mutations (loss of function or missense variants)  
18 was observed. Because no deleterious *BMP7* mutations (loss of function or missense variants)  
19 was observed. Because no deleterious *BMP7* mutations (loss of function or missense variants)  
20 was observed. Because no deleterious *BMP7* mutations (loss of function or missense variants)  
21 was observed. Because no deleterious *BMP7* mutations (loss of function or missense variants)  
22 was observed. Because no deleterious *BMP7* mutations (loss of function or missense variants)  
23 was observed. Because no deleterious *BMP7* mutations (loss of function or missense variants)  
24 was observed. Because no deleterious *BMP7* mutations (loss of function or missense variants)  
25 was observed. Because no deleterious *BMP7* mutations (loss of function or missense variants)  
26 was observed. Because no deleterious *BMP7* mutations (loss of function or missense variants)  
27 was observed. Because no deleterious *BMP7* mutations (loss of function or missense variants)  
28 was observed. Because no deleterious *BMP7* mutations (loss of function or missense variants)  
29 was observed. Because no deleterious *BMP7* mutations (loss of function or missense variants)  
30 was observed. Because no deleterious *BMP7* mutations (loss of function or missense variants)  
31 was observed. Because no deleterious *BMP7* mutations (loss of function or missense variants)  
32 was observed. Because no deleterious *BMP7* mutations (loss of function or missense variants)  
33 was observed. Because no deleterious *BMP7* mutations (loss of function or missense variants)  
34 was observed. Because no deleterious *BMP7* mutations (loss of function or missense variants)  
35 was observed. Because no deleterious *BMP7* mutations (loss of function or missense variants)  
36 was observed. Because no deleterious *BMP7* mutations (loss of function or missense variants)  
37 was observed. Because no deleterious *BMP7* mutations (loss of function or missense variants)  
38 was observed. Because no deleterious *BMP7* mutations (loss of function or missense variants)  
39 was observed. Because no deleterious *BMP7* mutations (loss of function or missense variants)  
40 was observed. Because no deleterious *BMP7* mutations (loss of function or missense variants)  
41 was observed. Because no deleterious *BMP7* mutations (loss of function or missense variants)  
42 was observed. Because no deleterious *BMP7* mutations (loss of function or missense variants)  
43 was observed. Because no deleterious *BMP7* mutations (loss of function or missense variants)  
44 was observed. Because no deleterious *BMP7* mutations (loss of function or missense variants)  
45 was observed. Because no deleterious *BMP7* mutations (loss of function or missense variants)  
46 was observed. Because no deleterious *BMP7* mutations (loss of function or missense variants)  
47 was observed. Because no deleterious *BMP7* mutations (loss of function or missense variants)  
48 was observed. Because no deleterious *BMP7* mutations (loss of function or missense variants)  
49 was observed. Because no deleterious *BMP7* mutations (loss of function or missense variants)  
50 was observed. Because no deleterious *BMP7* mutations (loss of function or missense variants)  
51 was observed. Because no deleterious *BMP7* mutations (loss of function or missense variants)  
52 was observed. Because no deleterious *BMP7* mutations (loss of function or missense variants)  
53 was observed. Because no deleterious *BMP7* mutations (loss of function or missense variants)  
54 was observed. Because no deleterious *BMP7* mutations (loss of function or missense variants)  
55 was observed. Because no deleterious *BMP7* mutations (loss of function or missense variants)  
56 was observed. Because no deleterious *BMP7* mutations (loss of function or missense variants)  
57 was observed. Because no deleterious *BMP7* mutations (loss of function or missense variants)  
58 was observed. Because no deleterious *BMP7* mutations (loss of function or missense variants)  
59 was observed. Because no deleterious *BMP7* mutations (loss of function or missense variants)  
60 was observed. Because no deleterious *BMP7* mutations (loss of function or missense variants)  
61 was observed. Because no deleterious *BMP7* mutations (loss of function or missense variants)  
62 was observed. Because no deleterious *BMP7* mutations (loss of function or missense variants)  
63 was observed. Because no deleterious *BMP7* mutations (loss of function or missense variants)  
64 was observed. Because no deleterious *BMP7* mutations (loss of function or missense variants)  
65 was observed. Because no deleterious *BMP7* mutations (loss of function or missense variants)

48 We also performed luciferase assays to assess the regulatory activity of rs6127972, the  
49 non-imputed SNP observed to have the strongest association with mNCS. To conduct the assays,  
50 we generated 667-bp fragments (chr20:55,796,885-55,797,557, hg19) with either the G allele or T  
51 allele of rs6127972 and containing a nearby DNaseI hypersensitivity cluster (chr20:55,797,206-  
52 55,797,555, hg19). These fragments were cloned 5' upstream of a *BMP7* promoter reporter  
53  
54  
55  
56  
57  
58  
59  
60  
61  
62  
63  
64  
65

construct (Figure 3). The expression of the luciferase reporter for both fragments with either with the risk (T) or common (G) allele at rs6127972 was significantly lower compared to the empty control vector (Figure 3). Although the trend for expression levels was consistent with the T allele (over-transmitted in our mNCS sample) having the lowest expression, the two allele fragments did not differ significantly in their modulation of promoter activity ( $P = 0.05$ ). After adjustment for multiple tests, both fragments compared to the empty control were significant (G allele  $P = 3.78 \times 10^{-5}$ ; T allele  $P = 5.11 \times 10^{-6}$ ), suggesting the region around rs6127972 may act as a repressor element. The control luciferase experiment with the randomly selected fragments of 667 bp flanking rs1857502 did no change the expression of the luciferase reporter. This corroborates our observation of inhibitory effect of rs6127972 as locus specific (Figure 3b).

Our imputation analysis identified a linkage disequilibrium block (chr20:55,790,147-55,807,110, hg19) encompassing rs6127972 and rs162319 (the most significant association to mNCS) containing several regulatory elements. These regulatory elements included several annotated enhancers. One of these enhancers overlaps a CTCF transcription factor binding site, and we found this region (chr20:55,798,821-55,798,917) to be significantly hypomethylated in MSCs derived from fused metopic sutures compared to those from open sutures from the same proband, suggesting stronger binding at this site (Figure 4). Further investigation of the other SNPs in the linkage disequilibrium block and regulatory elements in the region may be warranted.

## Discussion

Our GWAS of 215 NHW case-parent triads identified several loci associated with mNCS at a genome-wide significance level, but only the association with rs6127972 was replicated in an independent case-control sample. Of the SNPs that did not replicate, rs781716 is intronic to

1  
2  
3  
4 *SPRY3*, which is a modulator of FGF signaling (Panagiotaki et al. 2010) and has been suggested  
5  
6 as a candidate for autism (Ning et al. 2015); rs62590971 is ~155 kb upstream from *TGIF2LX*,  
7  
8 which plays a role in spermatogenesis (Wang et al. 2008); and the remaining three SNPs  
9  
10 (rs2522623, rs2573826, rs2754857) are all located intronic to *PCDH11X*, which has been  
11  
12 suggested to play a role in cognition related disorders (Veerappa et al. 2013). Whole exome  
13  
14 sequencing (WES) of 136 cases with mNCS and 237 cases with sNCS did not report rare variants  
15  
16 in *SPRY3*, *TGIF2LX*, or *PCDH11X* (Timberlake et al. 2017), and a WES of 191 cases with either  
17  
18 mNCS or sNCS did not report any mutations in *SPRY3* (Timberlake et al. 2016).  
19  
20  
21  
22

23  
24 Our discovery sample of 215 NHW case-parent triads had a 5:1 ratio of male to female  
25  
26 cases, and when we restricted analysis of X chromosome SNPs to those with allele frequency  
27  
28 differences  $< 0.15$  between males and females (quality control threshold for analysis was  $< 0.2$ ),  
29  
30 only the association with rs62590971 was significant (allele frequency difference between males  
31  
32 and females equal to 0.099). Differences in allelic frequency, especially in unbalanced samples  
33  
34 like ours, can lead to apparent over-transmission of one or the other allele to the affected offspring  
35  
36 (Loley et al. 2011). Lack of any strong association signal in our replication sample to these pseudo-  
37  
38 autosomal regions suggests that the associations in our discovery sample might have been a result  
39  
40 of allele frequency differences between males and females. Based on this finding and available  
41  
42 data from the literature, *SPRY3*, *TGIF2LX*, and *PCDH11X* have not been currently identified as  
43  
44 genetic factors involved in the development of mNCS.  
45  
46  
47  
48  
49

50  
51 The one SNP, rs6127972, replicated in our mNCS GWAS is intronic to *BMP7*, a member  
52  
53 of the BMP superfamily. This superfamily is involved in skeletal development (Beederman et al.  
54  
55 2013; Salazar et al. 2016) by inducing bone formation (Asahina et al. 1996; Fujii et al. 1999) and  
56  
57 may have therapeutic potential for orthopedic applications (Salazar et al. 2016). Developmental  
58  
59  
60  
61  
62  
63  
64  
65

1  
2  
3  
4 abnormalities in the skull were identified in *Bmp7*-deficient mutant mice, including fusion of the  
5  
6 basisphenoid with the occipital bone.(Luo et al. 1995). Enhanced BMP signaling through BMP  
7  
8 type IA receptor in neural crest cells produces CS in mice (Komatsu et al. 2013). Rapamycin  
9  
10 rescues BMP-mediated midline CS through the inhibition of mTOR signaling in mice (Kramer et  
11  
12 al. 2018). Importantly, our sNCS GWAS documented a strong and reproducible association with  
13  
14 rs1884302 located 345 kb downstream of *BMP2* (Justice et al. 2012), and our functional analysis  
15  
16 demonstrated that this locus may act as an enhancer element (Justice et al. 2017). Loss of function  
17  
18 mutations were identified in *SMAD6*, a negative regulator of the BMP signaling pathway, in cases  
19  
20 with midline CS, and a two-locus inheritance with synergistic effect of *SMAD6* loss of function  
21  
22 mutations with the C allele of rs1884302 was suggested (Timberlake et al. 2016). Our findings for  
23  
24 mNCS further implicate the BMP signaling pathway in the development of CS.  
25  
26  
27  
28  
29  
30

31 In summary, our GWAS identified a variant in *BMP7*, rs6127972, which was significantly  
32  
33 and reproducibly associated with mNCS. Results from our luciferase assays suggest that the  
34  
35 intronic *BMP7* region containing this SNP could act as a repressor element, as both the risk and  
36  
37 common allele reduced expression of the *BMP7* promoter that was not observed in our control  
38  
39 luciferase assay. Even with these results, it is possible that the 667 bp fragment may regulate  
40  
41 another gene in the region, including an uncharacterized gene ~6kb away LOC102723590;  
42  
43 however, given our phenotype (premature ossification of a suture), we considered *BMP7* as a  
44  
45 candidate due to its role in bone development. Previous work has shown *BMP7* to be involved in  
46  
47 skeletal development (Beederman et al. 2013; Salazar et al. 2016), and along with the findings  
48  
49 from our study and previous reports (Justice et al. 2012; Kramer et al. 2018; Whitton et al. 2016),  
50  
51 suggests some role for BMP signaling in CS. Additionally, our meta-analysis of GWAS data for  
52  
53 mNCS and sNCS identified rs10262453 (intronic to *BBS9*) appears to be involved with midline  
54  
55  
56  
57  
58  
59  
60  
61  
62  
63  
64  
65

1  
2  
3  
4 NCS. Future efforts to examine whether the allele at rs10262453, or the regulatory region  
5  
6 surrounding it, interacts with *BMP2* and/or *BMP7*, or acts independently by regulating another  
7  
8 gene involved in suture formation are warranted.  
9

10  
11  
12  
13  
14 **Financial disclosure statement:** On behalf of all authors, the corresponding author states that  
15  
16 there is no conflict of interest.  
17  
18  
19  
20

21 **Acknowledgements** The authors thank all families who contributed to this study. This project was  
22  
23 supported by the: National Institute of Dental and Craniofacial Research (NIDCR)/National  
24  
25 Institutes of Health (NIH) R01 DE016886 (S.A.B., P.A.R., A.C., K.B.); NIDCR/NIH DE018277  
26  
27 (M.L.C.); Centers for Disease Control and Prevention cooperative agreements under PA #96043,  
28  
29 PA #02081, FOA #DD09-001, FOA #DD13-003, and NOFO #DD18-001 to the Centers for Birth  
30  
31 Defects Research and Prevention participating in the National Birth Defects Prevention Study  
32  
33 and/or the Birth Defects Study To Evaluate Pregnancy exposureS and the Iowa Center for Birth  
34  
35 Defects Research and Prevention U01 DD001035 and U01 DD001223 (P.A.R.); Wellcome  
36  
37 Investigator Award 102731 (A.O.M.W.); the Università Cattolica del Sacro Cuore (W.L.); and in  
38  
39 part, by the Division of Intramural Research Program of the National Human Genome Research  
40  
41 Institute, NIH (C.M.J., J.A.S., A.F.W.). Additional support was provided by the Intramural  
42  
43 Research Program, National Institute of Child Health and Human Development, NIH:  
44  
45 HHSN275201100001I, HHSN27500005. We thank Samantha Edwards, Gill Roberts, Danielle  
46  
47 Stevenson, Vivienne Sutton, Elizabeth Tidey, Paolo Frassanito, Luca Massimi and Massimo  
48  
49 Caldarelli for help with specimen collection. Genotyping services were provided by the Center for  
50  
51 Inherited Disease Research (CIDR). CIDR is fully funded through a federal contract from the NIH  
52  
53  
54  
55  
56  
57  
58  
59  
60  
61  
62  
63  
64  
65

to The Johns Hopkins University, contract number HHSN268200782096C. The findings and conclusions in the report are those of the authors and do not necessarily represent the official position of the Centers for Disease Control and Prevention.

## References

- Altarac M, Saroha E (2007) Lifetime prevalence of learning disability among US children. *Pediatrics* 119 Suppl 1: S77-83. doi: 10.1542/peds.2006-2089L
- Asahina I, Sampath TK, Hauschka PV (1996) Human osteogenic protein-1 induces chondroblastic, osteoblastic, and/or adipocytic differentiation of clonal murine target cells. *Exp Cell Res* 222: 38-47. doi: 10.1006/excr.1996.0005
- Beederman M, Lamplot JD, Nan G, Wang J, Liu X, Yin L, Li R, Shui W, Zhang H, Kim SH, Zhang W, Zhang J, Kong Y, Denduluri S, Rogers MR, Pratt A, Haydon RC, Luu HH, Angeles J, Shi LL, He TC (2013) BMP signaling in mesenchymal stem cell differentiation and bone formation. *J Biomed Sci Eng* 6: 32-52. doi: 10.4236/jbise.2013.68A1004
- Benjamini Y, Hochberg Y (1995) Controlling the False Discovery Rate: A Practical and Powerful Approach to Multiple Testing. *Journal of the Royal Statistical Society. Series B* 57: 289-300.
- Chang X, Wang K (2012) wANNOVAR: annotating genetic variants for personal genomes via the web. *J Med Genet* 49: 433-6. doi: 10.1136/jmedgenet-2012-100918
- Cohen MM, MacLean RE (2000) *Craniosynostosis : diagnosis, evaluation, and management*, 2nd edn. Oxford University Press, New York
- Cordell HJ (2002) Epistasis: what it means, what it doesn't mean, and statistical methods to detect it in humans. *Hum Mol Genet* 11: 2463-8.
- Das S, Forer L, Schonherr S, Sidore C, Locke AE, Kwong A, Vrieze SI, Chew EY, Levy S, McGue M, Schlessinger D, Stambolian D, Loh PR, Iacono WG, Swaroop A, Scott LJ, Cucca F, Kronenberg F, Boehnke M, Abecasis GR, Fuchsberger C (2016) Next-generation genotype imputation service and methods. *Nat Genet* 48: 1284-1287. doi: 10.1038/ng.3656
- Delaneau O, Zagury JF, Marchini J (2013) Improved whole-chromosome phasing for disease and population genetic studies. *Nat Methods* 10: 5-6. doi: 10.1038/nmeth.2307
- Fujii M, Takeda K, Imamura T, Aoki H, Sampath TK, Enomoto S, Kawabata M, Kato M, Ichijo H, Miyazono K (1999) Roles of bone morphogenetic protein type I receptors and Smad proteins in osteoblast and chondroblast differentiation. *Mol Biol Cell* 10: 3801-13. doi: 10.1091/mbc.10.11.3801
- Greenwood J, Flodman P, Osann K, Boyadjiev SA, Kimonis V (2014) Familial incidence and associated symptoms in a population of individuals with nonsyndromic craniosynostosis. *Genet Med* 16: 302-10. doi: 10.1038/gim.2013.134
- Gupta PC, Foster J, Crowe S, Papay FA, Luciano M, Traboulsi EI (2003) Ophthalmologic findings in patients with nonsyndromic plagiocephaly. *J Craniofac Surg* 14: 529-32. doi: 10.1097/00001665-200307000-00026



- 1
  - 2
  - 3
  - 4
  - 5
  - 6
  - 7
  - 8
  - 9
  - 10
  - 11
  - 12
  - 13
  - 14
  - 15
  - 16
  - 17
  - 18
  - 19
  - 20
  - 21
  - 22
  - 23
  - 24
  - 25
  - 26
  - 27
  - 28
  - 29
  - 30
  - 31
  - 32
  - 33
  - 34
  - 35
  - 36
  - 37
  - 38
  - 39
  - 40
  - 41
  - 42
  - 43
  - 44
  - 45
  - 46
  - 47
  - 48
  - 49
  - 50
  - 51
  - 52
  - 53
  - 54
  - 55
  - 56
  - 57
  - 58
  - 59
  - 60
  - 61
  - 62
  - 63
  - 64
  - 65
- Howie B, Marchini J, Stephens M (2011) Genotype imputation with thousands of genomes. *G3* (Bethesda) 1: 457-70. doi: 10.1534/g3.111.001198
- Hunter AG, Rudd NL (1976) Craniosynostosis. I. Sagittal synostosis: its genetics and associated clinical findings in 214 patients who lacked involvement of the coronal suture(s). *Teratology* 14: 185-93. doi: 10.1002/tera.1420140209
- Jehee FS, Johnson D, Alonso LG, Cavalcanti DP, de Sa Moreira E, Alberto FL, Kok F, Kim C, Wall SA, Jabs EW, Boyadjiev SA, Wilkie AO, Passos-Bueno MR (2005) Molecular screening for microdeletions at 9p22-p24 and 11q23-q24 in a large cohort of patients with trigonocephaly. *Clin Genet* 67: 503-10. doi: 10.1111/j.1399-0004.2005.00438.x
- Justice CM, Kim J, Kim SD, Kim K, Yagnik G, Cuellar A, Carrington B, Lu CL, Sood R, Boyadjiev SA, Wilson AF (2017) A variant associated with sagittal nonsyndromic craniosynostosis alters the regulatory function of a non-coding element. *Am J Med Genet A* 173: 2893-2897. doi: 10.1002/ajmg.a.38392
- Justice CM, Yagnik G, Kim Y, Peter I, Jabs EW, Erazo M, Ye X, Ainehsazan E, Shi L, Cunningham ML, Kimonis V, Roscioli T, Wall SA, Wilkie AO, Stoler J, Richtsmeier JT, Heuze Y, Sanchez-Lara PA, Buckley MF, Druschel CM, Mills JL, Caggana M, Romitti PA, Kay DM, Senders C, Taub PJ, Klein OD, Boggan J, Zwienenberg-Lee M, Naydenov C, Kim J, Wilson AF, Boyadjiev SA (2012) A genome-wide association study identifies susceptibility loci for nonsyndromic sagittal craniosynostosis near BMP2 and within BBS9. *Nat Genet* 44: 1360-4. doi: 10.1038/ng.2463
- Kapp-Simon KA (1998) Mental development and learning disorders in children with single suture craniosynostosis. *Cleft Palate Craniofac J* 35: 197-203. doi: 10.1597/1545-1569\_1998\_035\_0197\_mdaldi\_2.3.co\_2
- Kazeem GR, Farrall M (2005) Integrating case-control and TDT studies. *Ann Hum Genet* 69: 329-35. doi: 10.1046/j.1529-8817.2005.00156.x
- Kent WJ, Sugnet CW, Furey TS, Roskin KM, Pringle TH, Zahler AM, Haussler D (2002) The human genome browser at UCSC. *Genome Res* 12: 996-1006. doi: 10.1101/gr.229102
- Komatsu Y, Yu PB, Kamiya N, Pan H, Fukuda T, Scott GJ, Ray MK, Yamamura K, Mishina Y (2013) Augmentation of Smad-dependent BMP signaling in neural crest cells causes craniosynostosis in mice. *J Bone Miner Res* 28: 1422-33. doi: 10.1002/jbmr.1857
- Kosoy R, Nassir R, Tian C, White PA, Butler LM, Silva G, Kittles R, Alarcon-Riquelme ME, Gregersen PK, Belmont JW, De La Vega FM, Seldin MF (2009) Ancestry informative marker sets for determining continental origin and admixture proportions in common populations in America. *Hum Mutat* 30: 69-78. doi: 10.1002/humu.20822
- Kramer K, Yang J, Swanson WB, Hayano S, Toda M, Pan H, Kim JK, Krebsbach PH, Mishina Y (2018) Rapamycin rescues BMP mediated midline craniosynostosis phenotype through reduction of mTOR signaling in a mouse model. *Genesis* 56: e23220. doi: 10.1002/dvg.23220
- Lajeunie E, Crimmins DW, Arnaud E, Renier D (2005) Genetic considerations in nonsyndromic midline craniosynostoses: a study of twins and their families. *J Neurosurg* 103: 353-6. doi: 10.3171/ped.2005.103.4.0353
- Lajeunie E, Le Merrer M, Bonaiti-Pellie C, Marchac D, Renier D (1995) Genetic study of nonsyndromic coronal craniosynostosis. *Am J Med Genet* 55: 500-4. doi: 10.1002/ajmg.1320550422

- Lajeunie E, Le Merrer M, Bonaiti-Pellie C, Marchac D, Renier D (1996) Genetic study of scaphocephaly. *Am J Med Genet* 62: 282-5. doi: 10.1002/(SICI)1096-8628(19960329)62:3<282::AID-AJMG15>3.0.CO;2-G
- Lattanzi W, Barba M, Novegno F, Massimi L, Tesori V, Tamburrini G, Galgano S, Bernardini C, Caldarelli M, Michetti F, Di Rocco C (2013) Lim mineralization protein is involved in the premature calvarial ossification in sporadic craniosynostoses. *Bone* 52: 474-84. doi: 10.1016/j.bone.2012.09.004
- Lattanzi, W., Barba, M., Di Pietro, L. & Boyadjiev, S. A. Genetic advances in craniosynostosis. *Am J Med Genet A* **173**, 1406-1429, doi:10.1002/ajmg.a.38159 (2017).
- Livak KJ, Schmittgen TD (2001) Analysis of relative gene expression data using real-time quantitative PCR and the 2(-Delta Delta C(T)) Method. *Methods* 25: 402-8. doi: 10.1006/meth.2001.1262
- Loley C, Ziegler A, Konig IR (2011) Association tests for X-chromosomal markers--a comparison of different test statistics. *Hum Hered* 71: 23-36. doi: 10.1159/000323768
- Luo G, Hofmann C, Bronckers AL, Sohocki M, Bradley A, Karsenty G (1995) BMP-7 is an inducer of nephrogenesis, and is also required for eye development and skeletal patterning. *Genes Dev* 9: 2808-20.
- Magge SN, Westerveld M, Pruzinsky T, Persing JA (2002) Long-term neuropsychological effects of sagittal craniosynostosis on child development. *J Craniofac Surg* 13: 99-104. doi: 10.1097/00001665-200201000-00023
- McCarthy S, Das S, Kretschmar W, Delaneau O, Wood AR, Teumer A, Kang HM, Fuchsberger C, Danecek P, Sharp K, Luo Y, Sidore C, Kwong A, Timpson N, Koskinen S, Vrieze S, Scott LJ, Zhang H, Mahajan A, Veldink J, Peters U, Pato C, van Duijn CM, Gillies CE, Gandin I, Mezzavilla M, Gilly A, Cocca M, Traglia M, Angius A, Barrett JC, Boomsma D, Branham K, Breen G, Brummett CM, Busonero F, Campbell H, Chan A, Chen S, Chew E, Collins FS, Corbin LJ, Smith GD, Dedoussis G, Dorr M, Farmaki AE, Ferrucci L, Forer L, Fraser RM, Gabriel S, Levy S, Groop L, Harrison T, Hattersley A, Holmen OL, Hveem K, Kretzler M, Lee JC, McGue M, Meitinger T, Melzer D, Min JL, Mohlke KL, Vincent JB, Nauck M, Nickerson D, Palotie A, Pato M, Pirastu N, McInnis M, Richards JB, Sala C, Salomaa V, Schlessinger D, Schoenherr S, Slagboom PE, Small K, Spector T, Stambolian D, Tuke M, Tuomilehto J, Van den Berg LH, Van Rhee W, Volker U, Wijmenga C, Toniolo D, Zeggini E, Gasparini P, Sampson MG, Wilson JF, Frayling T, de Bakker PI, Swertz MA, McCarroll S, Kooperberg C, Dekker A, Altshuler D, Willer C, Iacono W, Ripatti S, et al. (2016) A reference panel of 64,976 haplotypes for genotype imputation. *Nat Genet* 48: 1279-83. doi: 10.1038/ng.3643
- Ning Z, McLellan AS, Ball M, Wynne F, O'Neill C, Mills W, Quinn JP, Kleinjan DA, Anney RJ, Carmody RJ, O'Keefe G, Moore T (2015) Regulation of SPRY3 by X chromosome and PAR2-linked promoters in an autism susceptibility region. *Hum Mol Genet* 24: 5126-41. doi: 10.1093/hmg/ddv231
- Panagiotaki N, Dajas-Bailador F, Amaya E, Papalopulu N, Dorey K (2010) Characterisation of a new regulator of BDNF signalling, Sprouty3, involved in axonal morphogenesis in vivo. *Development* 137: 4005-15. doi: 10.1242/dev.053173
- Purcell S, Neale B, Todd-Brown K, Thomas L, Ferreira MA, Bender D, Maller J, Sklar P, de Bakker PI, Daly MJ, Sham PC (2007) PLINK: a tool set for whole-genome association and population-based linkage analyses. *Am J Hum Genet* 81: 559-75. doi: 10.1086/519795

- Reefhuis J, Gilboa SM, Anderka M, Browne ML, Feldkamp ML, Hobbs CA, Jenkins MM, Langlois PH, Newsome KB, Olshan AF, Romitti PA, Shapira SK, Shaw GM, Tinker SC, Honein MA, National Birth Defects Prevention S (2015) The National Birth Defects Prevention Study: A review of the methods. *Birth Defects Res A Clin Mol Teratol* 103: 656-69. doi: 10.1002/bdra.23384
- Salazar VS, Gamer LW, Rosen V (2016) BMP signalling in skeletal development, disease and repair. *Nat Rev Endocrinol* 12: 203-21. doi: 10.1038/nrendo.2016.12
- Schwender H, Li Q, Neumann C, Taub MA, Younkin SG, Berger P, Scharpf RB, Beaty TH, Ruczinski I (2014) Detecting disease variants in case-parent trio studies using the bioconductor software package trio. *Genet Epidemiol* 38: 516-22. doi: 10.1002/gepi.21836
- Slater BJ, Lenton KA, Kwan MD, Gupta DM, Wan DC, Longaker MT (2008) Cranial sutures: a brief review. *Plast Reconstr Surg* 121: 170e-8e. doi: 10.1097/01.prs.0000304441.99483.97
- Tamburrini G, Caldarelli M, Massimi L, Santini P, Di Rocco C (2005) Intracranial pressure monitoring in children with single suture and complex craniosynostosis: a review. *Childs Nerv Syst* 21: 913-21. doi: 10.1007/s00381-004-1117-x
- Thompson DN, Harkness W, Jones B, Gonzalez S, Andar U, Hayward R (1995) Subdural intracranial pressure monitoring in craniosynostosis: its role in surgical management. *Childs Nerv Syst* 11: 269-75. doi: 10.1007/bf00301758
- Timberlake AT, Choi J, Zaidi S, Lu Q, Nelson-Williams C, Brooks ED, Bilguvar K, Tikhonova I, Mane S, Yang JF, Sawh-Martinez R, Persing S, Zellner EG, Loring E, Chuang C, Galm A, Hashim PW, Steinbacher DM, DiLuna ML, Duncan CC, Pelphrey KA, Zhao H, Persing JA, Lifton RP (2016) Two locus inheritance of non-syndromic midline craniosynostosis via rare SMAD6 and common BMP2 alleles. *Elife* 5. doi: 10.7554/eLife.20125
- Timberlake AT, Furey CG, Choi J, Nelson-Williams C, Yale Center for Genome A, Loring E, Galm A, Kahle KT, Steinbacher DM, Larysz D, Persing JA, Lifton RP (2017) De novo mutations in inhibitors of Wnt, BMP, and Ras/ERK signaling pathways in non-syndromic midline craniosynostosis. *Proc Natl Acad Sci U S A* 114: E7341-E7347. doi: 10.1073/pnas.1709255114
- Veerappa AM, Saldanha M, Padakannaya P, Ramachandra NB (2013) Genome-wide copy number scan identifies disruption of PCDH11X in developmental dyslexia. *Am J Med Genet B Neuropsychiatr Genet* 162B: 889-97. doi: 10.1002/ajmg.b.32199
- Wang Y, Wang L, Wang Z (2008) Transgenic analyses of TGIF family proteins in *Drosophila* imply their role in cell growth. *J Genet Genomics* 35: 457-65. doi: 10.1016/S1673-8527(08)60063-6
- Whitton A, Hyzy SL, Britt C, Williams JK, Boyan BD, Olivares-Navarrete R (2016) Differential spatial regulation of BMP molecules is associated with single-suture craniosynostosis. *J Neurosurg Pediatr* 18: 83-91. doi: 10.3171/2015.12.PEDS15414
- Willer CJ, Li Y, Abecasis GR (2010) METAL: fast and efficient meta-analysis of genomewide association scans. *Bioinformatics* 26: 2190-1. doi: 10.1093/bioinformatics/btq340
- Yoon PW, Rasmussen SA, Lynberg MC, Moore CA, Anderka M, Carmichael SL, Costa P, Druschel C, Hobbs CA, Romitti PA, Langlois PH, Edmonds LD (2001) The National Birth Defects Prevention Study. *Public Health Rep* 116 Suppl 1: 32-40. doi: 10.1093/phr/116.S1.32

1  
2  
3  
4  
5  
6  
7  
8  
9  
10  
11  
12  
13  
14  
15  
16  
17  
18  
19  
20  
21  
22  
23  
24  
25  
26  
27  
28  
29  
30  
31  
32  
33  
34  
35  
36  
37  
38  
39  
40  
41  
42  
43  
44  
45  
46  
47  
48  
49  
50  
51  
52  
53  
54  
55  
56  
57  
58  
59  
60  
61  
62  
63  
64  
65

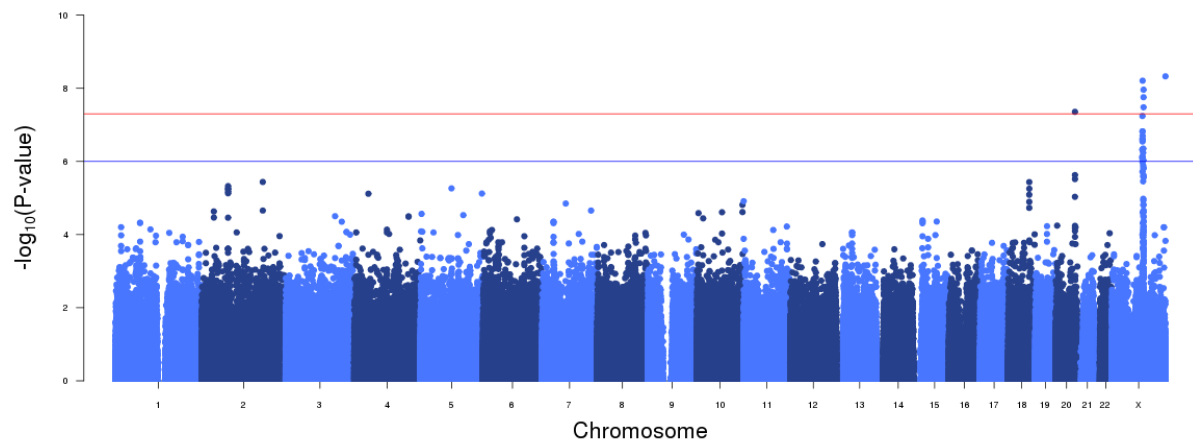
**Figure 1.** Plot of GWAS TDT  $P$ -values from analysis of 215 mNCS case-parent triads (649,669 SNPs). The values on the  $x$ -axis are the genomic positions of the markers, and the values on the  $y$ -axis are  $-\log_{10}$  of the  $P$ -values. The blue line represents the suggestive significance threshold of  $P \leq 1 \times 10^{-5}$ , whereas the red line represents a genome-wide significance threshold of  $P \leq 5 \times 10^{-8}$ .

**Figure 2.** Regional association plot and LD plot for association of rs6127972 to mNCS. (a)  $P$ -values ( $-\log_{10}$ ) of the GWAS are plotted against the genomic position of each SNP on chromosome 20 associated region ( $\pm 150$  kb from rs6127972), with genes in the region depicted below. The LD ( $r^2$ ) between rs6127972 and other SNPs are indicated with different colors. Recombination rate in cM per Mb using HapMap controls. (b) LD plot ( $r^2$ ) based on genotyped subjects (215 NHW case-parent triads).

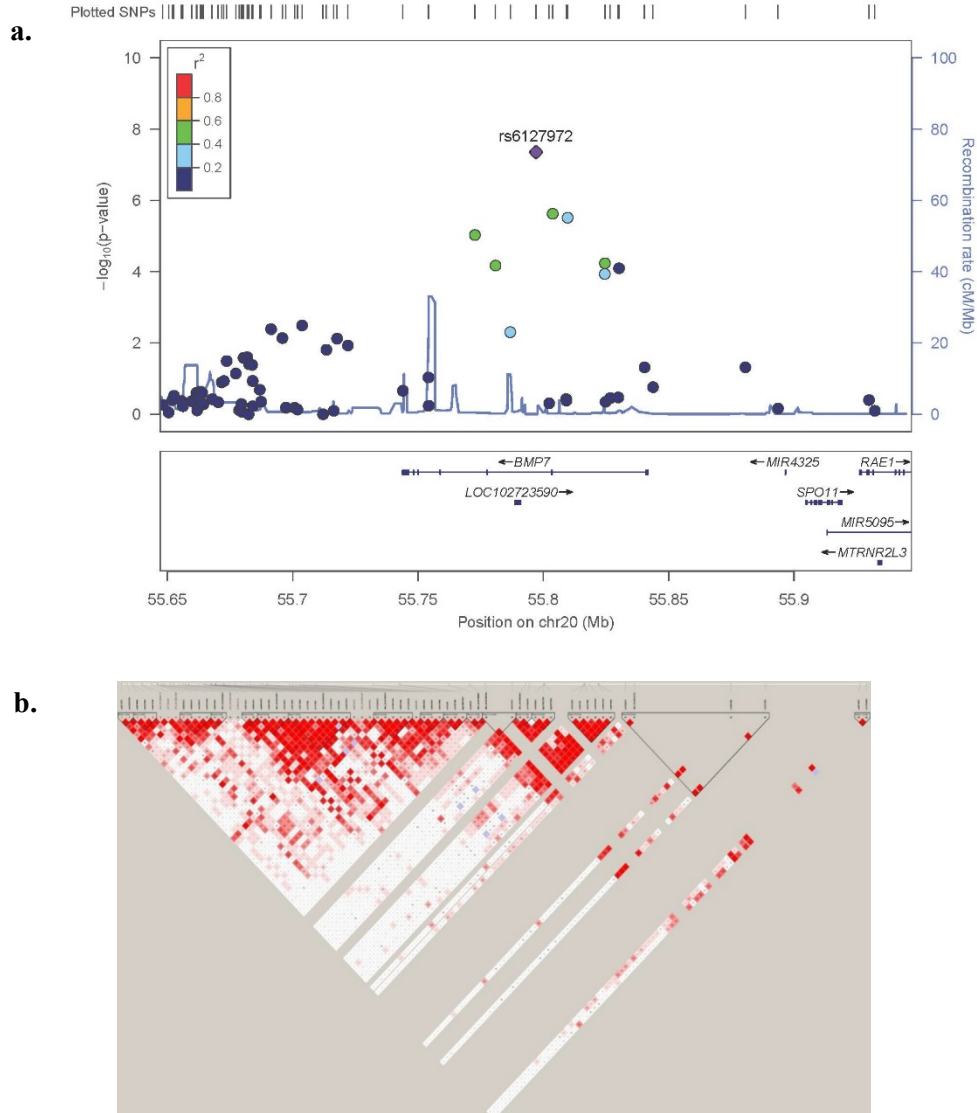
**Figure 3.** Luciferase assay of rs6127972 intronic to *BMP7*. (a) A 667 bp DNA fragment with either the common G allele or risk T allele at our GWAS significant SNP, rs6127972, were cloned at the RE position, 5' upstream of a BMP7 promoter reporter construct. Expression of the luciferase reporter for both fragments was significantly lower compared to the empty control (G allele  $P=3.78 \times 10^{-5}$ ; T allele  $P=5.11 \times 10^{-6}$ ). There was no statistically significant difference in the expression of the luciferase reporter between the G allele and T allele fragments ( $P=0.038$ ). (b) A randomly selected 667 bp DNA fragment with either G allele or T allele at rs1857502 (control fragment) was cloned at the RE position, 5' upstream of a BMP7 promoter reporter construct. Expression of the luciferase reporter for both fragments did not change compared to the empty control (G allele  $P=0.188$ ; T allele  $P=0.041$ ). (\*) represents significance at a level of 0.05 compared to the empty vector control. Bars represent mean  $\pm$  SE.

**Figure 4.** Average percent methylation of DNA isolated from 12 pairs of MSCs derived from fused metopic and open sutures from the same proband at three CpG sites. Of the seven CpG sites covered by the two sets of primers, three of the sites had 100% methylation across all specimens, and one site was extremely variable, so these sites were not analyzed further. Three sites (chr20:55,798,831-55,798,832,

chr20:55,798,857-55,798,858, chr20:55,798,873-55,798,874) were consistent across replicates and analyzed to determine any genotype- or phenotype-specific differences. No significant genotypic-specific differences were identified. There was a significant difference in methylation between the fused metopic and open sutures at the three analyzed sites, with *P*-values of  $6.4 \times 10^{-6}$ ,  $1.39 \times 10^{-5}$ , and 0.012, respectively.

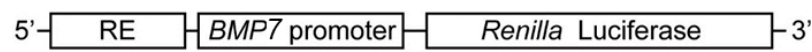


GWAS, genome-wide association study; mNCS, metopic nonsyndromic craniosynostosis; SNP, single nucleotide polymorphism; TDT, transmission disequilibrium test.

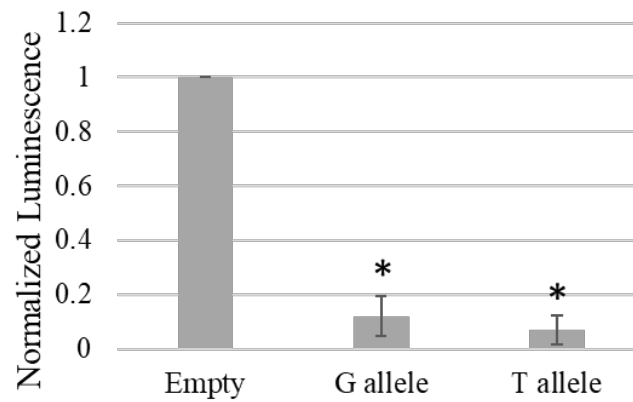


cM centimorgan; GWAS, genome-wide association study; LD, linkage disequilibrium; Mb, megabase; mNCS, metopic nonsyndromic craniosynostosis; NHW, non-Hispanic White; SNP, single nucleotide polymorphism.

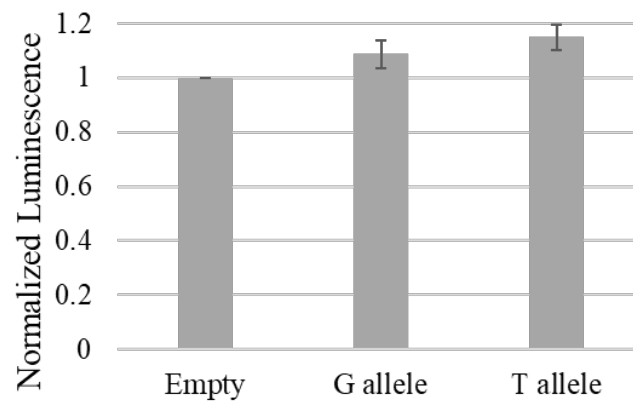




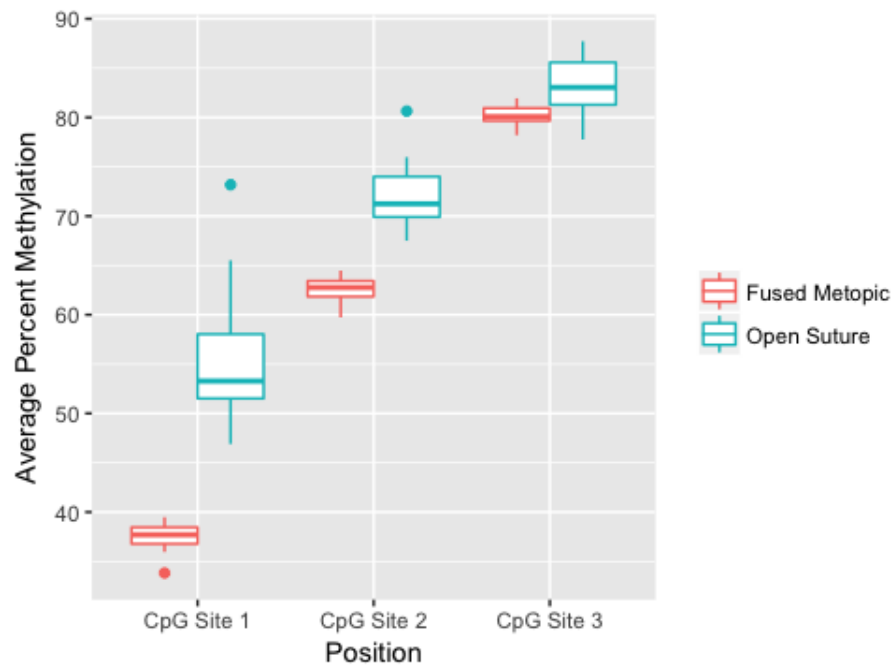
**a**



**b**



(\*) represents significance at a level of  $P < 0.05$  compared to the empty vector control. Bars represent mean  $\pm$  SE.  
 bp, base pair; GWAS, genome-wide association study; RE, regulatory element; SNP, single nucleotide polymorphism.



MSCs, mesenchymal stem cells. The control sites were consistent across replicates and showed no significant differences in percent methylation between the fused and open sutures.